

# Computer simulations of dense hard-sphere systems

M. D. Rintoul and S. Torquato

Princeton Materials Institute and Department of Civil Engineering and Operations Research,  
Princeton University, Princeton, New Jersey 08540

(Received 24 June 1996; accepted 22 August 1996)

We present comprehensive results of large-scale molecular dynamics and Monte Carlo simulations of systems of dense hard spheres at volume fraction  $\phi$  along the disordered, metastable branch of the phase diagram from the freezing-point  $\phi_f$  to random close packing volume  $\phi_c$ . It is shown that many previous simulations contained deficiencies caused by crystallization and finite-size effects. We quantify the degree of local crystallization through an order parameter and study it as a function of time and initial conditions to determine the necessary conditions to obtain truly random systems. This ordering criterion is used to show that previous methods employed to ascertain the degree of randomness are inadequate. A careful study of the pressure is also carried out along the entire metastable branch. In the vicinity of the random-close packing fraction, we show that the pressure scales as  $(\phi_c - \phi)^{-\gamma}$ , where  $\gamma = 1$  and  $\phi_c = 0.644 \pm 0.005$ . Contrary to previous studies, we find no evidence of a thermodynamic glass transition. © 1996 American Institute of Physics.  
[S0021-9606(96)51044-5]

## I. INTRODUCTION

Random packings of hard spheres have received considerable attention since they serve as a useful model for a number of physical systems, such as simple liquids,<sup>1</sup> glasses,<sup>2</sup> colloidal dispersions and particulate composites.<sup>3</sup> The hard-sphere model turns out to approximate well the structure of dense-particle systems with more complicated potentials (e.g., Leonard-Jones interactions) because short-range repulsion between the particles is primarily responsible for determining the spatial arrangement of the particles.

Despite the simplicity of the hard-spheres potential, there is strong numerical evidence for the existence of a first-order disorder/order phase transition.<sup>4</sup> There are four important branches shown in the phase diagram (Fig. 1), where the pressure is plotted versus the sphere volume fraction  $\phi = 4\pi a^3 \rho / 3$ , with  $\rho$  and  $a$  being the number density and radius of the spheres, respectively. There is a fluid branch that starts at  $\phi = 0$  and continues up to the freezing-point volume fraction,  $\phi_f$ , which occurs at approximately  $\phi_f \approx 0.494$ . At this point, the phase diagram splits into two parts. One part is a metastable extension of the fluid branch which follows continuously from the previous branch and is conjectured to end at a point known as *random close packing*. This state can be defined as the *maximum* packing fraction over all ergodic ensembles at which the mean nearest neighbor distance  $\lambda$  is equal to the sphere diameter  $\sigma$ .<sup>5</sup> Extensive numerical work indicates that the volume fraction  $\phi_c$  of the random close-packed state is approximately 0.64.<sup>6</sup> The other branch that splits off the freezing point represents the thermodynamically stable part of the phase diagram. Along the horizontal portion of this branch (tieline) both fluid and solid can coexist until the melting point  $\phi_m \approx 0.545$  is reached. The portion of the curve which continues above the melting point is referred to as the solid or ordered branch, ending at the close-packed fcc crystal at a volume fraction of  $\sqrt{2}\pi/6 = 0.7405 \dots$ , which is the maxi-

um volume fraction for a packing of spheres in three dimensions.

The fact that the hard-sphere system freezes is somewhat remarkable at first glance since there are no attractive interparticle interactions. In order to understand the existence of the phase transition one must look at the difference in entropy (i.e., the number of available states) in the ordered system versus the disordered system.<sup>7</sup> For low densities, there are a very large number of disordered states in which the spheres can arrange themselves compared with the number of ordered states. This difference causes the fluid system to be thermodynamically stable. For larger and larger values of the density, the disordered configurations pack less and less efficiently, causing there to be increasingly fewer allowable disordered configurations. However, at the higher densities, the decrease in the number of ordered states is much less significant. At some point, there are many more ordered states than disordered states, and the system freezes. This is also often described in terms of the “configurational entropy” decreasing rapidly as a function of packing fraction, while the “communal entropy” decreases at a much slower rate.<sup>4</sup>

There are many difficulties one encounters when simulating the hard-sphere system at high densities. It is difficult to construct systems of spheres above  $\phi_f$ , since one cannot melt a crystal at high densities and expect it to spontaneously go into the metastable phase. One must start with a system at a lower density and carefully “compress” the fluid, being cautious not to allow crystallization to occur. Therefore, in order to study the properties in the system, it must be evolved in time while still remaining on the disordered metastable branch. There is currently no explicit test for determining whether or not the system is on the metastable branch of the phase diagram. Imprecise methods such as looking for peaks associated with the fcc crystal in the radial distribution function are often used to determine whether the system has left the metastable branch.<sup>8,9</sup> Unfortunately, this method does

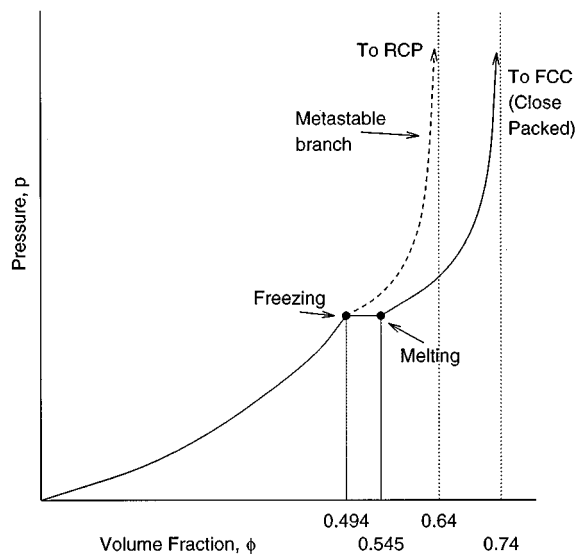


FIG. 1. Phase diagram in the pressure-volume fraction plane for the hard-sphere system.

not have the resolution necessary to deal with small amounts of crystallization for very dense amorphous systems. In these “supercooled” systems, small amounts of crystallization can dramatically change the behavior of the system, especially near random close packing.

One of the most studied phenomena in amorphous systems is that of the so-called “glass transition.”<sup>2,10</sup> It is the general phrase used to describe the effect of a precipitous change in a macroscopic property of the system (e.g., diffusion coefficient). In hard-sphere systems, previous investigations<sup>9,11,12</sup> have found that a thermodynamic glass transition supposedly exists at a density  $\phi_g$ , where  $\phi_f \leq \phi_g \leq \phi_c$ . However, it is still an open question as to whether this transition is a true thermodynamic phase transition, or just a continuous change in the dynamic variables caused by the increase in density. If it is a second-order phase transition, as many believe, very precise values of the pressure must be calculated in order for it to be seen. This emphasizes even more the necessity of being able to precisely tell when the system is in the metastable state, the crystalline state, or somewhere in between.

In order to determine the pressure precisely and answer the questions posed above, we plan to carry out the following investigations:

- (1) We test whether or not the radial distribution function  $g(r)$  is a sensitive measure of the occurrence of crystallization in the system.
- (2) We employ a quantitative measure of the local order to probe for signs of crystallization.
- (3) A precise calculation of the pressure as a function of  $\phi$  along the metastable branch, i.e.,  $\phi_f \leq \phi < \phi_c$ , is performed using the aforementioned measure of local order as a guide to minimize crystallization.
- (4) We perform a careful study to determine whether precise

values of the pressure really indicate a true phase transition at densities near the supposed glass transition.

- (5) We carry out an asymptotic study of how the pressure in the system diverges near random close packing and compare it to previous works.

In Sec. II, we discuss the difficulties in obtaining very dense systems of random hard spheres, and define the quantities that will be used to characterize the systems that we study. We describe the computational details in Sec. III and present our results in Sec. IV. Section V contains a discussion of our results and their implications. Finally, we present our conclusions in Sec. VI.

## II. OBTAINING DENSE EQUILIBRIUM HARD-SPHERE SYSTEMS

Most techniques that are used to create random dense hard-sphere (RDHS) systems (e.g., above a volume fraction of about 0.5) create non-equilibrium systems. However, we are interested in an equilibrium RDHS system which, along the metastable branch ( $\phi_f \leq \phi \leq \phi_c$ ), will generally have significantly different properties than the non-equilibrium systems. In theory, it is a simple matter to equilibrate RDHS systems using simple molecular dynamics (MD) or Monte Carlo (MC) techniques, but in practice this is very difficult in the study of random systems. The process of going from the initial non-equilibrium RDHS system to the equilibrium RDHS system is *fundamental* to the study of RDHS systems. This has generally not been noted by previous studies in which more attention was paid to the algorithm which creates the system than to the equilibration process.

The question of equilibration is a subtle one because there are two phenomena which are occurring simultaneously during the equilibration process for the range  $\phi_f \leq \phi \leq \phi_c$ . The first is that of the system moving from the non-equilibrium state to a final equilibrium state. However, at the same time, the RDHS system is crystallizing. This is due to the fact that the equilibrium RDHS system is metastable, and further evolution of the system moves the system toward the stable branch of the dense hard-sphere system which is the crystalline branch for densities above the melting-point volume fraction  $\phi_m$  (see Fig. 1). The time scale for the non-equilibrium to metastable equilibrium transition  $\tau_m$  is generally shorter than the time scale related to the transition from the metastable to the stable ordered branch,  $\tau_c$ , i.e.,  $\tau_c \gg \tau_m$ . However, these time scales can be similar to each other in some cases, and vary depending on the density of the system and the nature of the initial non-equilibrium system.

Accordingly, it is important that the systems be carefully monitored during the equilibration process. The most important property of the system is the pressure. Initially, this is usually much higher in the non-equilibrium configurations created by most algorithms which involve a “quenching” procedure, so there is a steady, exponential-like decay of the pressure as the system settles into the equilibrium state. As the system begins to crystallize the pressure drops further. This drop in pressure is not as smooth as that due to the

equilibration process. It is sometimes characterized by sharp drops, especially at densities close to RCP, caused by the sudden crystallization of parts of the system. At densities further from RCP, the transition into crystalline order tends to be a more continuous process. In either case, the effects can become mixed with those of the pressure drop during equilibration.

Previous studies have attempted to determine the onset of crystallization by studying the radial distribution function (RDF).<sup>9</sup> The radial distribution function is defined as

$$g(r) = \frac{\rho^{(2)}(r)}{\rho^2}, \quad (1)$$

where  $\rho^{(2)}(r)$  is the two-particle density function, and  $\rho$  is just the density in the system. Effectively, the radial distribution function measures the extent to which the position of the particle centers deviates from that of an uncorrelated ideal gas. As crystallization begins to occur, a very small peak begins to appear for values of  $r$  which correspond to the next nearest neighbor in the fcc lattice. For a close packed system, this occurs at  $r/\sigma = \sqrt{2}$ , but for the small crystallites that appear in the random system it occurs at approximately  $r/\sigma \approx 1.5$ . This is due to the fact that the spheres are not necessarily touching, but are just locally arranged in the crystalline configuration. Previous investigators assumed that there was no crystallization if the peak was not seen. This method is very unsatisfying since the lack of its appearance does not necessarily mean that crystallization is not occurring and it is difficult to determine exactly when this peak appears.

Steinhardt, Nelson, and Ronchetti<sup>13</sup> have proposed a more quantitative measure of local order in the system that is often used in studies of crystallization. First, one must define a set of bonds connecting neighboring spheres in the system. In this case, the definition of a neighbor could be any sphere within a specified radius, or a neighbor in the sense of sharing a face of a Wigner–Seitz cell. One then assigns the value

$$Q_{lm}(\mathbf{r}) \equiv Y_{lm}(\theta(\mathbf{r}), \phi(\mathbf{r})) \quad (2)$$

to each bond oriented in a direction  $\mathbf{r}$ , where the  $Y_{lm}$  are the spherical harmonics. These values are then averaged over all bonds to get

$$\overline{Q_{lm}} \equiv \langle Q_{lm}(\mathbf{r}) \rangle. \quad (3)$$

The quantity  $\overline{Q_{lm}}$ , for a specific  $l$  and  $m$ , is dependent on the coordinate system but an invariant quantity  $Q_l$  can be obtained in the following manner:

$$Q_l \equiv \left( \frac{4\pi}{2l+1} \sum_{m=-l}^l |\overline{Q_{lm}}|^2 \right)^{1/2}. \quad (4)$$

We are specifically interested in  $Q_6$  which has the ideal property that it should be  $1/\sqrt{N_b}$ , where  $N_b$  is the number of bonds (see the appendix), for a completely random and spatially uncorrelated system (ideal gas). Moreover,  $Q_6$  is significantly larger for any type of crystallization, not just that associated with the fcc crystallization. The quantity  $Q_6$  is clearly a better signature of local order than the appearance

TABLE I. List of values for  $Q_6$  for various types of crystals. The values are for a bond definition which includes the nearest neighbors in all cases except for the bcc crystal, which contains next nearest neighbors.

| Geometry               | $Q_6$   |
|------------------------|---------|
| Icosahedral            | 0.66332 |
| Face-centered cubic    | 0.57452 |
| Hexagonal close packed | 0.48476 |
| Body-centered cubic    | 0.51059 |
| Simple cubic           | 0.35355 |

of the fcc nearest-neighbor peak in the RDF. Table I gives a list of the values of  $Q_6$  for various crystals. In a truly amorphous system there should be no crystallization of any sort, and this should be reflected in  $Q_6$ . Using all of this information, one can better judge whether the system is in a truly random state, or not.

### III. COMPUTATIONAL TECHNIQUES

The initial random dense hard-sphere (RDHS) systems were created using the technique described by Clarke and Wiley<sup>14</sup> (CW). In this algorithm one starts with an initial set of random overlapping spheres, and the spheres are expanded and simultaneously moved to reduce overlap. If the system becomes jammed to such an extent that it is difficult to reduce overlap, the spheres are shrunk a bit and moved around until the jamming condition is relieved. This process of expansion and contraction is repeated (with most of the moves being expansions) until a suitable volume fraction is reached.

This technique is somewhat different than that described by Stillinger, DiMarzio, and Kornegay,<sup>15</sup> or Jodrey and Tory<sup>16</sup> which only involve expansions. The CW algorithm can take a bit longer in some cases but is generally the fastest and most dependable way to create the large systems that we needed having volume fractions close to the RCP value. Once the other algorithms jam, there is no way to get the system any denser; so if one is trying to create very dense systems, the algorithm must be repeated over and over again until the density is reached. It is also important to note that the CW procedure starts with randomly distributed (i.e., overlapping) spheres. We have found that if one starts with an initial lattice configurations for spheres, remnants of this initial condition can often be seen in the final dense random configuration.

For the most part, the systems were equilibrated using standard hard-sphere molecular dynamics.<sup>17</sup> We found that this generally led to fast equilibration for the smaller systems. The time scale used in the figures is arbitrary, but is scaled in such a way that it was equivalent for systems of any number of particles. For some of the larger systems, a standard Metropolis Monte Carlo algorithm was used in the very large systems to equilibrate the systems. The other primary advantage of using the MD equilibration is that the pressure could be measured directly in addition to extrapolating the radial distribution function to  $r = \sigma$ , where it is to be recalled that  $\sigma$  is the sphere diameter. Unless otherwise specified, the

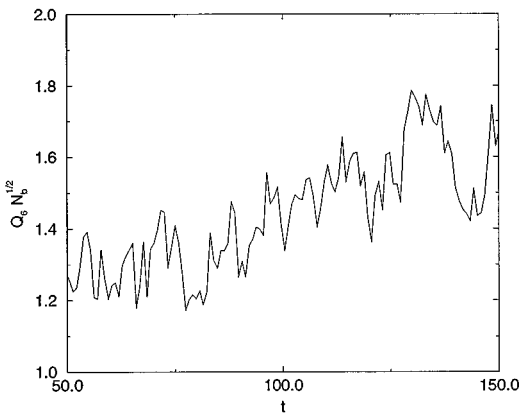


FIG. 2. Plot of  $Q_6 \times \sqrt{N_b}$  as a function of time in a random hard-sphere system at  $\phi=0.58$ , where  $N_b$  is the number of bonds in the system. There is a steady increase of  $Q_6$  as the system begins to crystallize. At very large times ( $t \approx 10^3 - 10^4$ ), the system eventually crystallizes.

number of spheres used for each simulation was 2000. This is significantly larger than many previous simulations which usually started with 500 or 864 spheres.

Unlike a system of particles interacting with a Leonard-Jones potential, the equilibrium hard-sphere system depends on the temperature  $T$  in a trivial manner. Assigning a higher initial value of the kinetic energy in one system compared to another effectively just rescales the time in the system. Indeed, it is well known that the reduced pressure  $Z = p/\rho k_B T$  (with  $k_B$  being Boltzman's constant) along the stable branches can be related to the value of the radial distribution function  $g(r)$  at contact ( $r = \sigma$ ) by the formula  $Z = 1 + 4\phi g(\sigma)$ , where  $\sigma$  is the diameter of the spheres. Therefore,  $Z$  depends only on the sphere volume fraction since  $g(\sigma)$  depends only on  $\phi$ .

## IV. RESULTS

### A. Effectiveness of $Q_6$ as a signature of local order

To illustrate the utility of  $Q_6$  as an appropriate signature of the local order in the system, we have plotted  $Q_6 \sqrt{N_b}$  vs  $t$  (Fig. 2), and the corresponding contact value  $g(\sigma)$  vs  $t$  (Fig. 3) for a system of dense random hard spheres at  $\phi=0.58$ . We plot  $Q_6 \sqrt{N_b}$  (instead of  $Q_6$ ) since this quantity for a finite spatially uncorrelated system is  $\approx 1$  (see the appendix). This normalized value also has the advantage that it helps remove the effect of having a different number of bonds for different samplings. This volume fraction was specifically chosen because it is close to the point at which many studies have noticed a discontinuity in the first derivative of the pressure as a function of volume fraction, i.e., a glass transition. The time does not start at 0, as we are trying to demonstrate the slow crystallization of an equilibrium random system, and not the equilibration of a non-equilibrium system. The contact value shows a steady drop, while the order parameter  $Q_6 \sqrt{N_b}$  shows a steady rise above its completely random value of approximately 1.0. As  $Q_6 \sqrt{N_b}$  approaches 2.0, there is significant disorder in the system, and the contact value is significantly changed from its value

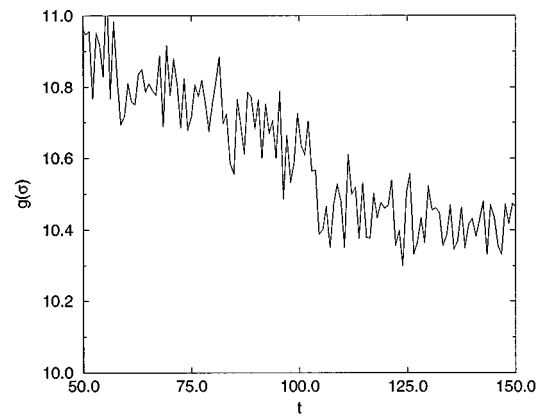


FIG. 3. Plot of the contact value of the RDF  $g(\sigma)$  as a function of time for a random hard sphere system at  $\phi=0.58$ . There is a steady decrease in the pressure as the system begins to crystallize.

when  $Q_6 \sqrt{N_b}$  was closer to 1.0. This gives clear evidence that there is some crystallization in the system. However, even if one closely examines the RDF for signs of a peak around 1.4–1.5, there is nothing to be seen. In fact, we have enlarged a plot of the RDF for that same system (Fig. 4) for various times that are associated with those in Fig. 2 and Fig. 3. We emphasize that even at this level of enlargement, the RDFs show no sign of a peak that would indicate crystallization.

A similar behavior is seen at other values of  $\phi$  above the freezing point  $\phi_f$ . The implication is that there is a constant rearrangement occurring in these systems which is driving the pressure down. The effect is seen in the RDF only after significant rearrangement has taken place.

### B. Measurement of the contact value as a function of volume fraction along the metastable branch up to RCP

Using the specific techniques mentioned in the previous sections that carefully established when the RDHS system was in the random equilibrium state, we show the values of

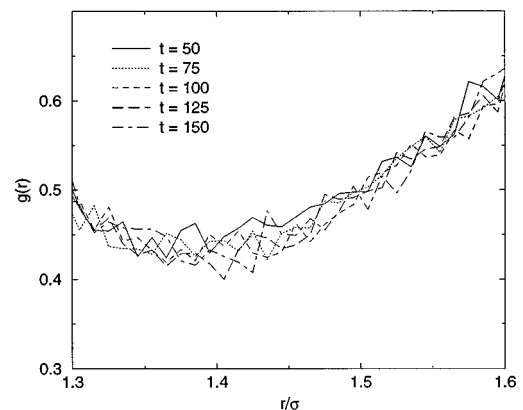


FIG. 4. Enlarged portion of the RDF of the system shown in Figs. 2 and 3. There is no sign of the peak that many studies associate with crystallization.

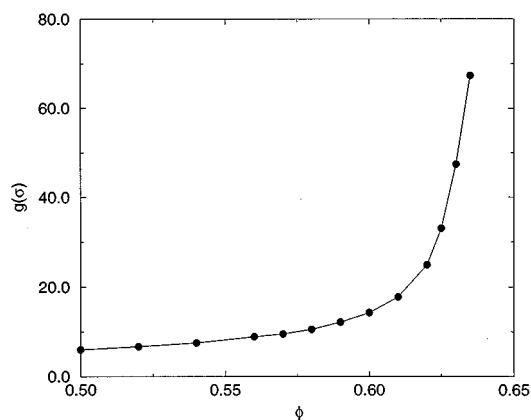


FIG. 5. Plot of simulation data for the equilibrium contact value  $g(\sigma)$  of dense random hard-sphere systems. The data points are joined by straight lines.

the contact value plotted against the density in the system in Fig. 5, and the numerical values are given in Table II. The pressure in the case of these points is that plotted from the virial calculated using MD methods. The curve shows a steady increase, but does not show a discontinuity in the derivative as would be expected from a second-order phase transition.

Using this data, we can now also test what the behavior of  $g(\sigma)$  should be as  $\phi \rightarrow \phi_c$ . There is strong numerical evidence that  $g(\sigma)$  diverges as  $(\phi_c - \phi)^{-\alpha}$  as  $\phi \rightarrow \phi_c$ . By fitting our data for  $\phi \geq 0.60$  on a log-log plot, we found that  $\alpha \approx 1$ , within the errors of our simulation. This fit is shown with the data in Fig 6. An extrapolation to  $g(\sigma)^{-1} = \infty$  gives a value of  $0.644 \pm 0.005$  for  $\phi_c$ .

## V. DISCUSSION

### A. Detection of order in hard-sphere systems

There is clearly a need for more a quantitative determination of order and disorder in hard-sphere systems. Although the method we have outlined is only partially quan-

TABLE II. Table of the contact value  $g(\sigma)$  as a function of density. These values were determined using the virial computed from a molecular dynamics simulation.

| $\phi$ | $g(\sigma)$ |
|--------|-------------|
| 0.50   | 6.00        |
| 0.52   | 6.71        |
| 0.54   | 7.53        |
| 0.56   | 8.90        |
| 0.57   | 9.57        |
| 0.58   | 10.6        |
| 0.59   | 12.2        |
| 0.60   | 14.3        |
| 0.61   | 17.8        |
| 0.62   | 25.0        |
| 0.625  | 33.1        |
| 0.63   | 47.4        |
| 0.635  | 67.4        |

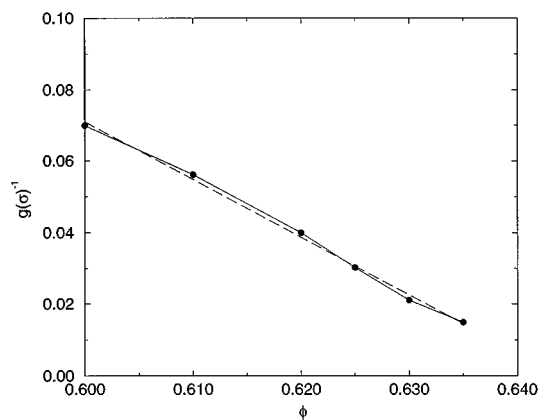


FIG. 6. Plot of  $g(\sigma)^{-1}$  vs  $\phi$  for  $\phi \geq 0.60$ . The dashed line is the best fit assuming  $g(\sigma) \propto (\phi_c - \phi)^{-1}$ . The value extrapolates down to an  $x$ -intercept of  $\phi = 0.644 \pm 0.005$ .

titative, it clearly shows the inadequacy of simply equilibrating and then looking for the existence of a peak near  $r/\sigma = 1.5$ . Ideally, one would like to be able to calculate analytically what the value of  $Q_6$  should be for a system of random hard spheres at volume fraction  $\phi$ , as one can for Poisson spheres. This is especially important at volume fractions close to  $\phi_c$ , where the pressure approaches infinity, and any small amount of crystallization in the system could cause significant fluctuations in that value.

### B. The question of the existence of the glass transition

The argument for the existence of the glass transition in a system of hard spheres is usually based on the fact that in simulations, it is often found that when a system is brought to a dense state by quickly expanding the spheres (or “quenching”), it does not crystallize for long periods of equilibration. It is then supposed that the system is locked into the amorphous state and cannot reach the crystalline state. After performing many such equilibrations, we have found that this effect is primarily due to *system size*. By performing equilibrations between melting  $\phi_m$  and random close packing  $\phi_c$ , we have found that if one waits for long enough times (typically  $10^7 - 10^8$  collisions in some cases), the systems will eventually equilibrate and crystallize. Figure 7 illustrates this important point for a system of 2000 spheres at  $\phi = 0.58$ , where  $Q_6$  is small for small times (indicating high disorder) and large for large times (indicating crystallization).  $Q_6$  is not exactly zero at  $t = 0$  since the system is not infinitely large and because of short range correlations. At large times,  $Q_6$  does not take on the value of the fcc crystal for two reasons. First, the crystal is not close-packed at that volume fraction and the particles are not located in the exact crystal locations. Second, the 2000-particle crystal in an environment with periodic cubic boundary conditions does not have the correct number of particles to form a perfect crystal. We emphasize that crystallization occurred even for systems very close to  $\phi_c$  ( $\phi \approx 0.63 - 0.64$ ). We have encountered many smaller systems that do not crystallize, but most of

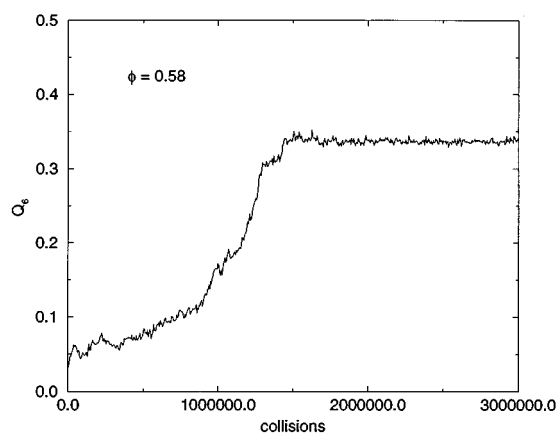


FIG. 7. Plot of the unnormalized  $Q_6$  as a function of collisions for a system of 2000 particles at  $\phi=0.58$ . Note that the final value of  $Q_6$  is not that of a fcc crystal because the particles are not close packed in a perfect crystal, and also because a 2000 particle fcc crystal with periodic cubic boundary conditions will necessarily have some imperfections.

these had at most 500 particles. Once the system size was on the order of 2000–5000 particles, crystallization usually occurred at shorter time scales.

Interestingly, recent Shuttle experiments of hard-sphere colloidal dispersions carried out in microgravity showed a very similar crystallization behavior for volume fractions between  $\phi_m=0.545$  and  $\phi=0.62$ .<sup>18</sup> These systems consisted of approximately  $2 \times 10^{13}$  PMMA spheres of diameter  $0.518 \mu\text{m}$ , which supports our point that finite-size effects keep smaller systems from crystallizing. (Of course, hydrodynamic effects in the Shuttle experiment are ignored in our simulations, albeit under the absence of gravity.) Similar experiments done under normal surface gravity indicate that crystallization does not occur for RDHS systems that have densities which are roughly between  $\phi_m$  and  $\phi_c$ .

It is also possible to see why previous simulations were perhaps able to see a change in the first derivative of the pressure as a function of density for values of  $\phi$  close to where they thought a second-order phase transition existed. We first note that at a volume fraction of approximately  $\phi=0.59$ , we noticed that the time required for metastable equilibrium  $\tau_m$  was greater than that of the time required for crystallization  $\tau_c$ . The value of the pressure in this case had to be determined by looking at times at which crystallization had not yet occurred and extrapolation of those values for long times, assuming an exponential decay to a final value. We tried this for other volume fractions and found it gave accurate values for the pressure of the RDHS systems, given short-time values. We believe that the fact that the crystallization time scale is so short in this case is the main cause for a belief that there is a “transition” near this volume fraction. The pressure calculated at this volume fraction in most simulations contains significant crystallization and therefore the measured pressure is too low. It is also important to mention that even if the pressure is measured carefully within the region around  $\phi=0.59$ , the errors associated with the pressure measurement are really still too large to say conclu-

sively that a transition does exist since the second derivative is also increasing rapidly along with the first derivative.

### C. Behavior of $g(\sigma)$ as $\phi \rightarrow \phi_c$

Our results  $\phi_c=0.644 \pm 0.005$  and  $\alpha \approx 1$  are somewhat similar to previous numerical results, but do clear up some discrepancies between them. Tobochnik and Chapin<sup>19</sup> studied the behavior of  $g(\sigma)$  for  $\phi$  near  $\phi_c$  and arrived at the values  $\alpha=1$  and  $\phi_c=0.69$ . This paper was of special interest as they performed their simulations on the surface of a four-dimensional hypersphere, in order to inhibit crystallization. Their value of  $\phi_c$  is much larger than the results given by most other simulations of  $\phi_c \approx 0.64$ . However, the systems studied in that paper contained less than 500 spheres (although they also used data from Woodcock<sup>20</sup> which used 500 sphere systems). *Perhaps more important, the precise value of  $g(\sigma)$  was much more difficult to establish.* This was due to the fact that they were using a MC equilibration scheme and had to evaluate  $g(\sigma)$  by extrapolating the contact value from the values of the bins near  $r=\sigma$ . Their bin size was  $0.02\sigma$ , so the error of extrapolation is significant, especially at densities near  $\phi_c$  when the RDF is increasing rapidly near  $r=\sigma$ . We also tried to use the extrapolation method to obtain a value of  $g(\sigma)$  to compare with the virial method, and found that much care had to be taken for the extrapolation near RCP, and this was even the case when we were using our smaller bin widths. They used a quadratic fit for their extrapolation, which becomes increasingly inadequate as the pressure diverges.

Song *et al.*<sup>21</sup> also attempted to evaluate  $\alpha$  and  $\phi_c$ , using data from Alder and Wainwright,<sup>17</sup> and Erpenbeck and Wood.<sup>22</sup> They obtained a value of  $\phi_c=0.6435$  and a value of  $\alpha=0.76 \pm 0.02$ . This value of  $\phi_c$  is much more in line with previous estimates as well as our estimate. The error associated with their estimate of  $\alpha$  did not seem to be derived in a systematic way, and it was probably much too small. We note here that any attempt to evaluate  $\alpha$  numerically with any great precision would involve knowing extremely accurate values of the pressure for densities very close to random close packing. This accuracy would require much larger systems to avoid any problems of finite-size effects, and would also require a *microscopic* measure of disorder to exclude any effects of crystallization.

### D. Comparison of the contact value method and virial method for measuring pressure

As we noted before, we calculated both the pressure using both the contact value, where  $Z=1+4\phi g(\sigma)$ , and by measuring the pressure directly through the interparticle collisions (virial method). The two methods are well known to be equivalent for stable equilibrium systems, but it is not clear that these arguments hold for densities above freezing in which the system lies along the metastable branch. Under close inspection, we have found the two to be equivalent for the entire metastable branch. For densities above  $\phi \approx 0.62$ , the comparison is made difficult by the fact that  $g(r)$  is

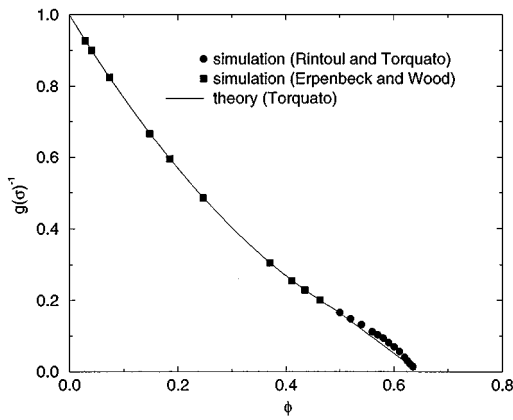


FIG. 8. Plot of  $g(\sigma)^{-1}$  vs  $\phi$  for  $0 \leq \phi \leq \phi_c$ . The circles represent data from this work, the squares represent data from Erpenbeck and Wood (Ref. 22), and the line represents the theoretical curve from Torquato (Ref. 5).

increasing rapidly as  $r \rightarrow \sigma^+$ , but if the RDF is scaled by  $(r/\sigma)^\nu$ , where  $\nu$  is some appropriately chosen large integer, the extrapolation is much easier.

### E. Behavior of $g(\sigma)$ for $0 \leq \phi \leq \phi_c$

By using the values obtained in this study, along with the very precise values of the pressure obtain by Erpenbeck and Wood,<sup>22</sup> we can compare the analytical predictions of Torquato<sup>5</sup> for values of  $g(\sigma)$  for  $0 \leq \phi \leq \phi_c$ , given by

$$g(\sigma) = a_0 + a_1 + a_2, \quad (5)$$

where

$$a_0 = 1 + 4\phi g_f(\sigma) \frac{(\phi_c - \phi_f)}{\phi_c - \phi}, \quad (6)$$

$$a_1 = \frac{3\phi - 4}{2(1 - \phi)} + 2(1 - 3\phi) g_f(\sigma) \frac{(\phi_c - \phi_f)}{\phi_c - \phi}, \quad (7)$$

$$a_2 = \frac{2 - \phi}{2(1 - \phi)} + (2\phi - 1) g_f(\sigma) \frac{(\phi_c - \phi_f)}{\phi_c - \phi}, \quad (8)$$

and  $g_f(\sigma)$  is just  $g(\sigma)$  evaluated at  $\phi_f$ . Note that the theoretical prediction has precisely the same asymptotic form near  $\phi_c$  as our numerical estimate, i.e.,  $g(\sigma)$  scales as  $(\phi_c - \phi)^{-1}$  as  $\phi \rightarrow \phi_c$ . Figure 8 shows  $g(\sigma)^{-1}$  shows the simulation data plotted against the theoretical curve, where values of  $\phi_c = 0.644 \pm 0.005$  and  $\phi_f = 0.49$  were used as parameters for the theoretical curve. The theory matches very well with the simulation for  $\phi < \phi_f$ . For  $\phi_f \leq \phi \leq \phi_c$ , the curve diverges somewhat from the theory for values of  $\phi$  outside the immediate vicinity of the random close-packing volume fraction  $\phi_c$  since it assumes a first-order pole for all  $\phi_f \leq \phi \leq \phi_c$ . Although the theory matches reasonably well for densities above the freezing density, the true behavior of the system is too complex to be completely captured by a first-order pole. In the immediate vicinity of  $\phi_c$ , however, the theory is highly accurate, as expected.

## VI. CONCLUSIONS

We have established, in a quantitative way, a means of testing for local order in a system of dense hard spheres. By using this technique, we are not only able to establish when the system is truly random, but have also shown that previous methods of looking for the next-nearest-neighbor peak in the RDF are not precise enough. Using this technique, we have measured precise values of the contact value  $g(\sigma)$  for the hard sphere system on the metastable branch for values  $\phi_m \leq \phi < \phi_c$ . With these new accurate results, we see no evidence of a second-order phase transition in the vicinity of the so called ‘‘glass transition.’’ We also find that  $g(\sigma)$  diverges near RCP as  $(\phi_c - \phi)^{-1}$ , where  $\phi_c = 0.644 \pm 0.005$ . We do not see any indication of a fractal exponent, as indicated by earlier studies.

## ACKNOWLEDGMENTS

The authors thank R. Speedy, G. Grest, P. Debenedetti, P. Chaikin, and J. Zhu for useful conversations. We gratefully acknowledge the Office of Basic Energy Sciences, U.S. Department of Energy under Grant No. DE-FG02-92ER14275 for their support of this work.

## APPENDIX: BEHAVIOR OF $Q_6$ FOR A SPATIALLY UNCORRELATED SYSTEM

To determine the behavior of the  $Q_l$  for spatially uncorrelated systems, let us examine each  $|Q_{lm}|^2$  in detail. By definition, we have

$$|\overline{Q_{lm}}|^2 = \left| \frac{1}{N_b} \sum_i Y_{lm}(\theta_i, \phi_i) \right|^2 \quad (A1)$$

$$= \frac{1}{N_b^2} \sum_i |Y_{lm}(\theta_i, \phi_i)|^2 + \frac{1}{N_b^2} \sum_{b_i \neq j} Y_{lm}(\theta_i, \phi_i) Y_{lm}^*(\theta_j, \phi_j). \quad (A2)$$

Now for a truly random set of bonds (where the bond angles are distributed uniformly around a unit sphere), a sum over random angles of a function  $F(\mathbf{r}_i)$  is equivalent to an integration over all angles, i.e.,

$$\lim_{N_b \rightarrow \infty} \left( \frac{1}{N_b} \sum_{b_i=1}^{N_b} F(\mathbf{r}_i) \right) = \frac{\int d\Omega F(\mathbf{r})}{\int d\Omega}. \quad (A3)$$

Using the conditions that

$$\int d\Omega |Y_{lm}(\theta_i, \phi_i)|^2 = 1 \quad (A4)$$

and

$$\int d\Omega Y_{lm}(\theta_i, \phi_i) = 0 \quad (A5)$$

the first term on the left hand side of Eq. (A2) becomes  $1/4\pi N_b$  and the second term is 0, so we have

$$|\overline{Q_{lm}}|^2 = \frac{1}{4\pi N_b}. \quad (\text{A6})$$

Substituting this into Eq. (4), we get

$$Q_l = 1/\sqrt{N_b}. \quad (\text{A7})$$

This is the rate at which the order parameter  $Q_l$  should go to zero for a completely random system of points. The expected width of the fluctuations in  $Q_l$  can also be calculated in a similar manner so that for an average measure of  $Q_l$  for a system of  $N_b$  bonds, one should get:

$$Q_l = \frac{1}{\sqrt{N_b}} \pm \frac{1}{\sqrt{4l+2}} \frac{1}{\sqrt{N_b}}. \quad (\text{A8})$$

This expression holds for any definition of the bonds, assuming they are not spatially correlated.

<sup>1</sup>J. P. Hansen and I. R. McDonald, *Theory of Simple Liquids* (Academic, London, 1986).

<sup>2</sup>R. Zallen, *The Physics of Amorphous Solids* (Wiley, New York, 1983).

<sup>3</sup>S. Torquato and F. Lado, *Phys. Rev. B* **33**, 6428 (1986).

<sup>4</sup>W. G. Hoover and F. H. Ree, *J. Chem. Phys.* **49**, 3609 (1968).

<sup>5</sup>S. Torquato, *Phys. Rev. E* **51**, 3170 (1995).

<sup>6</sup>J. G. Berryman, *Phys. Rev. A* **27**, 1053 (1983).

<sup>7</sup>H. Reiss and A. D. Hammerich, *J. Phys. Chem.* **90**, 6252 (1986).

<sup>8</sup>W. S. Jodrey and E. M. Tory, *Powder Technol.* **30**, 111 (1981).

<sup>9</sup>R. J. Speedy, *J. Chem. Phys.* **100**, 6684 (1994).

<sup>10</sup>R. M. Ernst, S. R. Nagel, and G. S. Grest, *Phys. Rev. B* **43**, 8070 (1991).

<sup>11</sup>J. Yeo, *Phys. Rev. E* **52**, 853 (1995).

<sup>12</sup>A. van Blaaderen and P. Wiltzius, *Science* **270**, 1177 (1995).

<sup>13</sup>P. J. Steinhardt, D. R. Nelson, and M. Ronchetti, *Phys. Rev. B* **28**, 784 (1983).

<sup>14</sup>A. S. Clarke and J. D. Wiley, *Phys. Rev. B* **35**, 7350 (1987).

<sup>15</sup>F. H. Stillinger, E. A. DiMarzio, and R. L. Kornegay, *J. Chem. Phys.* **40**, 1564 (1964).

<sup>16</sup>W. S. Jodrey and E. M. Tory, *Phys. Rev. A* **32**, 2347 (1985).

<sup>17</sup>B. J. Alder and T. E. Wainwright, *J. Chem. Phys.* **33**, 1439 (1960).

<sup>18</sup>J. Zhu, M. Li, W. B. Russel, P. M. Chaikin, R. Rogers, and W. Meyers (unpublished).

<sup>19</sup>J. Tobochnik and P. M. Chapin, *J. Chem. Phys.* **88**, 5824 (1988).

<sup>20</sup>L. V. Woodcock, *Ann. N. Y. Acad. Sci.* **37**, 274 (1981).

<sup>21</sup>Y. Song, R. M. Stratt, and E. A. Mason, *J. Chem. Phys.* **88**, 1126 (1988).

<sup>22</sup>J. J. Erpenbeck and W. W. Wood, *J. Stat. Phys.* **35**, 321 (1984).